Metallophysics and Advanced Technologies
Металофіз. новітні технол.
Metallofiz. Noveishie Tekhnol.
2026, vol. 48, No. 9, pp. 963–972
https://doi.org/10.15407/mfint.48.09.0963
Reprints available directly from the publisher

© 2026 G. V. Kurdyumov Institute for Metal Physics,
National Academy of Sciences of Ukraine
Published by license under
the G. V. Kurdyumov Institute for Metal Physics–
N.A.S. of Ukraine Publishers imprint.
Printed in Ukraine.

PACS numbers: 61.72.Ff, 62.20.Qp, 62.23.Pq, 68.37.Hk, 81.20.Ev, 81.40.Jj, 81.70.Bt

Synthesis and Characterization of a Ti_3SiC_2–TiC–$TiSi_2$ Composite for High-Temperature Applications

I. M. Kirian[*], A. M. Lakhnik[*], M. A. Skoryk[*], S. O. Kotrechko[*], O. V. Zatsarna[*], T. O. Monastyrska[*], I. V. Gurin[**], and O. D. Rud[*]

[*]*G. V. Kurdyumov Institute for Metal Physics, N.A.S. of Ukraine, 36 Academician Vernadsky Blvd., UA-03142 Kyiv, Ukraine*
[**]*Institute of Solid State Physics, Materials Science and Technologies, NSC 'KIPT', 1 Akademichna Str., UA-61108 Kharkiv, Ukraine*

The influence of sintering conditions (pressure and holding time) on the structure and mechanical properties of Ti–Si–C-system composites is investigated. A formation of the Ti_3SiC_2, TiC, and $TiSi_2$ phases in the composite is confirmed by XRD analysis. Structural parameters of individual phases and mechanical characteristics of the obtained composites are determined. As found, samples S2 and S3 have superior compressive strength (σ_u) of 1445 MPa and 1460 MPa, respectively. At the same time, sample S3 demonstrates the highest hardness of ≅ 10.5 GPa (1072 *HV*), significantly outperforming the values obtained for S1 (≅ 6.7 GPa, 689 *HV*) and S2 (≅ 6.5 GPa, 677 *HV*).

Key words: Ti_3SiC_2, MAX phase, composite, XRD.

Досліджено вплив умов спікання (тиску та часу витримки) на структуру та механічні властивості композитів системи Ti–Si–C. Утворення фаз Ti_3SiC_2, TiC і $TiSi_2$ у композиті підтверджено за допомогою рентґеноструктурної аналізи. Визначено структурні параметри окремих фаз і механічні характеристики одержаних композитів. Виявлено, що зразки S2 і S3 ма-

Corresponding author: Oleksandr Rud
E-mail: rud@imp.kiev.ua

Citation: I. M. Kirian, A. M. Lakhnik, M. A. Skoryk, S. O. Kotrechko, O. V. Zatsarna, T. O. Monastyrska, I. V. Gurin, and O. D. Rud, Synthesis and Characterization of a Ti_3SiC_2–TiC–$TiSi_2$ Composite for High-Temperature Applications, *Metallofiz. Noveishie Tekhnol.*, **48**, No. 9: 963–972 (2026), DOI: 10.15407/mfint.48.09.0963

© Publisher PH 'Akademperiodyka' of the NAS of Ukraine, 2026. This is an open access article under the CC BY-ND license (https://creativecommons.org/licenses/by-nd/4.0)

ють вищу міцність на стиснення (σ_u) у 1445 МПа і 1460 МПа відповідно. Водночас, зразок S3 демонструє найвищу твердість у ≅ 10,5 ГПа (1072 *HV*), що значно перевершує значення, одержані для S1 (≅ 6,7 ГПа, 689 *HV*) і S2 (≅ 6,5 ГПа, 677 *HV*).

Ключові слова: Ti_3SiC_2, MAX-фаза, композит, рентґеноструктурна аналіза.

(Received 23 January, 2026; in final version, 23 July, 2026)

1. INTRODUCTION

Modern industry requires the creation of materials that are highly resistant to extreme conditions, such as high temperatures, aggressive environments, and significant mechanical loads. Therefore, researchers have recently focused on creating composite materials that will satisfy these conditions. Composites containing MAX phases open up new possibilities in the development of such materials. Ternary compounds with a layered hexagonal structure, known as MAX phases can meet these requirements and become excellent substitutes for high-temperature metals and ceramics. These materials are described by the generally accepted formula $M_{n+1}AX_n$ ($n = 1, 2, 3$), where M is a transition metal, A is the elements of the A-subgroup of the Mendeleev table and X = C or N [1–4]. The MAX phase of Ti_3SiC_2 has attracted practical interest for industrial applications. This phase has good physical and mechanical properties that meet the requirements of modern materials science. The Ti_3SiC_2 phase is characterized by high electrical ($4.5 \cdot 10^6$ $\Omega^{-1} \cdot m^{-1}$) and thermal conductivities (40–43 W/mK), low density ($\rho = 4.52$ g/cm^3), high Young's modulus ($E = 320$–343 GPa), flexural strength ≅ 260 MPa and compressive strength ≅ 580 MPa [5–8]. The melting point is ≅ 3000°C [4]. Further, the Ti_3SiC_2 MAX phase is characterized by a relatively insignificant coefficient of thermal expansion ≅ $9.1 \cdot 10^{-6}$ K^{-1} [9]. In addition, the Ti_3SiC_2 MAX phase is easily machinable and resistant to high-temperature oxidation. In works [10, 11], it is reported that the oxidation resistance of the MAX phase of Ti_3SiC_2 is maintained up to a temperature of ≅ 1000 °C. During the oxidation process of the MAX phase of Ti_3SiC_2, the formation of two oxide layers is observed. The outer layer contains anatase-type TiO_2. Increasing the oxidation duration leads to forming an inner layer containing two oxides, TiO_2 and SiO_2. One of the significant disadvantages among the mechanical properties of the MAX phase of Ti_3SiC_2 is its relatively low hardness, which is of ≅ 4 GPa (*HV*) [4]. This relatively modest hardness restricts its applicability in industry fields requiring high resistance to surface deformation or wear.

One of the promising approaches to solving this problem is the creation of composite materials based on MAX phases or with their content. Adding hard binary compounds (TiC or SiC) to the MAX phase

increases the hardness of the material. At the same time, the layered structure of MAX phases can provide composite materials with a high modulus of elasticity. All this makes MAX phases promising for many applications. An additional factor that positively affects the properties of composites is the introduction of $TiSi_2$ compounds into their composition. This additive helps increase the oxidation stability of the MAX phase of Ti_3SiC_2, which is important for applications in high temperatures and aggressive environments. Combining different phases in composites allows achieving an optimal balance between hardness, ductility, oxidation resistance, and other performance characteristics. Such composites are extremely promising for use in modern technologies that require materials with high mechanical and chemical properties.

The main purpose of this work was to study the influence of the phase composition and microstructure features on the mechanical properties of Ti_3SiC_2–TiC–$TiSi_2$ composites obtained by sintering the initial powder mixtures Ti–Si–C system. Special attention was paid to the relationship between the parameters of the sintering process and the evolution of the microstructure of composite materials.

2. MATERIALS AND METHODS

To synthesize Ti_3SiC_2–TiC–$TiSi_2$ composites, Ti (99.7%, $\cong$ 70 μm), Si (99.8%, $\cong$ 100 μm), and crystalline spectrally pure graphite (99.99% C, $\cong$ 50 μm) were used as starting materials. The powders were purchased from the commercial company 'GrandLada' (Kyiv, Ukraine). The initial powders of Ti, Si, and graphite were mixed in an atomic ratio of 3:1.1:2, respectively. Then, the mixture was homogenized on a laboratory planetary mill (Retsch PM100) at room temperature for 1 hour in a steel container. For mixing, 15 steel balls with a diameter of 10 mm were used. The rotational speed of the grinding container was of 200 rpm, and the balls-to-powder mass ratio was 20:1.

The homogenized powder mixtures were placed in a graphite mould with an internal diameter of 14 mm. The inner part of the mould and punch were separated from the sample with graphite foil. This prevented the sample from sintering with the mould parts at high temperatures. The all composite were sintered in an inert Ar atmosphere in a high-temperature furnace with an automated heating system developed at the G. V. Kurdyumov Institute for Metal Physics of the N.A.S. of Ukraine. Three types of samples were synthesized. The conditions for obtaining them are given in Table 1.

The x-ray diffraction (XRD) patterns were recorded using a powder diffractometer (DRON-4) in the Bragg–Brentano geometry with monochromatized MoK_α radiation (wavelength $\lambda = 0.71069$ Å). The x-ray diffraction patterns were processed by the Rietveld refinement tech-

TABLE 1. The sintering modes of the studied samples.

Sample	Sintering temperature, °C	Heating/cooling rate, K/min	Pressure, MPa	Holding time, min
S1	1385	50/150	60	30
S2*	1385	50/150	60	30 + 60
S3	1385	40/150	90	60

* The sample was synthesized by a two-stage sintering technique: holding at a temperature of 1385°C for 30 minutes and then cooling. Then, it was heated again and held at the same temperature for 60 minutes.

nique using the MAUD software [12]. Scanning electron microscopy (SEM) studies of the sintered composite were performed on a VEGA3 TESCAN microscope. Uniaxial compression tests were performed on an Instron 8802 universal servohydraulic testing machine. The hardness measurement was done using a Vickers indentation device on the polished surface of the composite sample with a load of 5000 g.

3. RESULTS AND DISCUSSION

Three samples were obtained for the study according to the conditions specified in Table 1. The synthesis of all samples took place at a temperature of 1385°C, with only the pressure and holding time at a given temperature change. Before the study, the samples were polished. The XRD phase identification of the sintered samples is shown in Fig. 1.

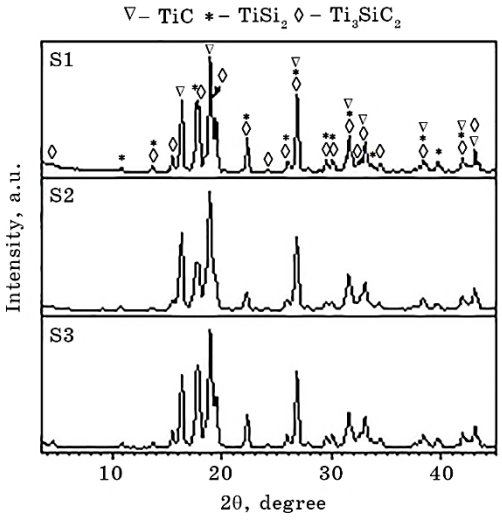


Fig. 1. Typical XRD patterns of the synthesized samples.

It is established that all synthesized samples mainly consist of three phases. The identified peaks are attributed for h.c.p. Ti_3SiC_2 (MAX phase), f.c.c. TiC, and orthorhombic $TiSi_2$ phases. The proportion of each phase in the sample was determined using Rietveld refinement. The result of the full-profile analysis is presented in Table 2. The sample S1 sintered at a pressure of 60 MPa with a holding time of 30 min contains approximately 25 wt.% Ti_3SiC_2 MAX phase, 41 wt.% TiC, and 34 wt.% $TiSi_2$.

The process of obtaining the sample S2 consisted of two stages of heat treatment. At the first stage, the sample was heated to a temperature of 1385°C and subjected to sintering under a pressure of 60 MPa for 30 minutes, which contributed to the initial formation of the phase composition. After completing this stage, the sample was quickly cooled to room temperature, which allowed it to reduce residual thermal stresses and stabilize its phase composition typical of sample S1. The first stage of obtaining S3 corresponds to the conditions for the synthesis of sample S1. In the second stage, the material was re-sintered at a similar pressure (60 MPa), but with an extension of the holding time to 60 minutes, which provided additional diffusion activity between the components and improved structural density. X-ray diffraction analysis revealed that the phase composition of sample S2 is similar to that of sample S1 (see Table 2). The absence of newly formed phases indicates the thermodynamic stability of the initial components under given conditions.

An increase in the sintering load to 90 MPa and the holding time to 60 min did not result in any changes to the phase composition of the sample (S3). X-ray phase analysis confirmed the preservation of the same crystalline phases as at lower sintering parameters. The content of each phase in S3 is comparable to samples S1 and S2. This indicates that with a further increase in load or holding time, the probability of

TABLE 2. Crystallographic parameters, phase percentage, and crystallite sizes acquired by Rietveld fitting from the XRD patterns of sintered samples.

Sample	Phase	Lattice parameters (Å)			Crystallite sizes (Å)	Abundance (wt.%)
		a	*b*	*c*		
S1	Ti_3SiC_2	3.065	–	17.677	570	25
	TiC	4.318	–	–	640	41
	$TiSi_2$	8.281	4.803	8.557	730	34
S2	Ti_3SiC_2	3.065	–	17.673	540	27
	TiC	4.317	–	–	730	40
	$TiSi_2$	8.279	4.803	8.557	820	33
S3	Ti_3SiC_2	3.064	–	17.664	480	24
	TiC	4.315	–	–	650	42
	$TiSi_2$	8.284	4.802	8.557	620	34

phase transformations remains minimal.

For all studied samples, the lattice parameters and crystallite size for each phase were calculated (Table 2). The results showed that the values of the lattice parameters for all samples remain practically identical, indicating the stability of the crystal structure when the synthesis conditions change. However, slight differences were found in the crystallite sizes, which may indicate some influence of different sintering parameters on the microstructure of the material. This may indicate an inhomogeneous phase distribution or the presence of defects in the material. The results obtained suggest that, although the lattice parameters are similar, the sintering conditions have an impact on the crystallite size, which, in turn, may influence the mechanical properties of the samples.

Figure 2 illustrates the SEM electron images in back-scattering electrons (BSE) mode taken from polished surface cross-section composites sintering at different conditions. SEM images demonstrate the heterogeneous structure of the material, consisting of dark and light areas. This indicates the presence of several phases with different chemical compositions in the composite.

A detailed microstructural analysis of the composites is shown in (Fig. 3). The MAX phase of Ti_3SiC_2 is represented by individual grains with a lamellar morphology, which can positively affect the mechanical plasticity of the material. The TiS_{i2} phase forms light gray intermetallic inclusions of rounded (sample S1, S2) or dendritic (sample S3) shape. According to the results of x-ray diffraction analysis, about 40 wt.% of the composite consists of titanium carbide (TiC). Thus, based on XRD data and microstructural studies, it was established that the composites formed by titanium carbide matrix with uniformly distributed inclusions of Ti_3SiC_2 and $TiSi_2$.

Energy dispersive x-ray spectral analysis (EDS) was used to perform a detailed analysis of the microstructure of the Ti_3SiC_2–TiC–$TiSi_2$

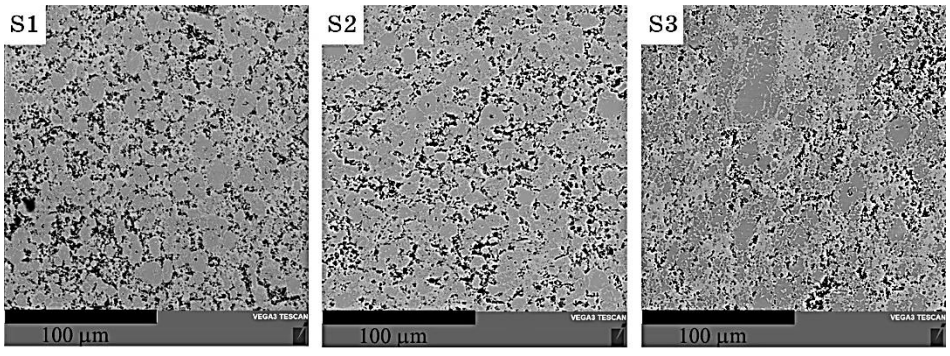


Fig. 2. Microstructure of bulk composite materials obtained after sintering.

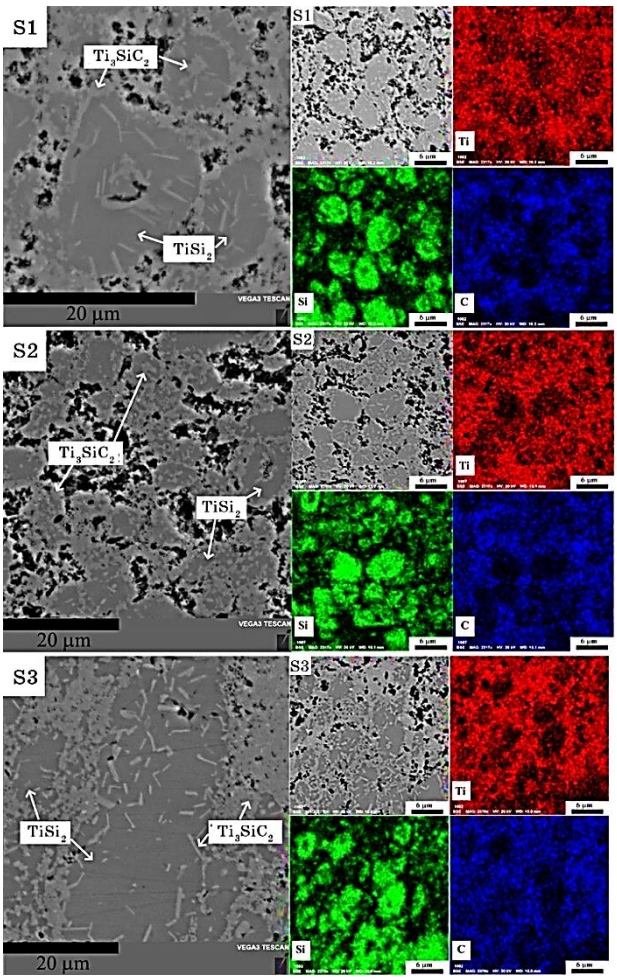


Fig. 3. Typical SEM micrographs of composite and element distribution maps.

composite and determine the distribution of its elemental composition. The use of EDS helps to identify possible inhomogeneities in the distribution of elements that may affect the performance characteristics of the composite. It is clear, the titanium and carbon are uniformly distributed over cross section of the sample.

The distribution of titanium on the elemental maps correlates with all three phases, while silicon is concentrated in the regions of the Ti_3SiC_2 and $TiSi_2$ phases. Carbon, as can be seen from its map, is mainly localized in TiC and in small amounts in areas typical of the Ti_3SiC_2 MAX phase. In the region responsible for the $TiSi_2$ phase, carbon is not observed. The overlap of the map areas with the most pronounced carbon and titanium concentrations indicates the dominant role of TiC in

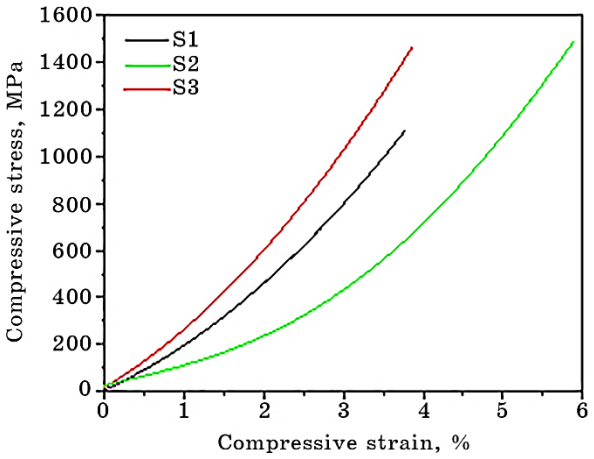


Fig. 4. Compressive stress–strain curves of synthesized composites.

the material structure. It is correlates well with the results of x-ray structure analysis. This microstructure provides an optimal combination of mechanical and thermal properties, which makes the material promising for applications in extreme operating conditions.

The effect of sample synthesis conditions on their mechanical properties was determined based on the results of uniaxial compression tests. The samples were brittle fractured without signs of macroplastic plastic deformation (Fig. 4). The values of compressive strength (σ_u) were determined and are given in Table 3. All samples contain a three-phase structure of Ti_3SiC_2, $TiSi_2$, and TiC significantly affecting their mechanical characteristics.

Sample S1 synthesized at a pressure of 60 MPa for 30 minutes demonstrate a compressive strength (σ_u) of 1096 MPa. Compared to other samples, this material has the lowest strength value. Relatively low strength values may be due to the insufficient duration of the sintering process, which did not ensure the full formation of interfacial bonds and led to residual porosity. In the case of sample S2, a two-stage sintering process, including initial heating at 60 MPa for 30 minutes, subsequent cooling, and repeated heating with a holding time of 60 minutes, contributes to the improvement of the mechanical properties of the material. For sample S2, the value σ_u is of 1460 MPa. The in-

TABLE 3. The mechanical properties of the studied samples.

Sample	Compressive strength (σ_u), MPa	Hardness, *HV*/GPa
S1	1096	689/6.7
S2	1460	677/6.5
S3	1445	1072/10.5

crease in the value σ_u may be because rapid cooling after the first heating stage contributed to the relaxation of residual stresses that arose during sintering. Reheating ensured improved diffusion processes, reduced the concentration of structural defects, and the formation of a more homogeneous microstructure, which together led to improved performance characteristics of the material. Sample S3 sintered at an elevated pressure of 90 MPa for 60 minutes demonstrated value of compressive strength $\sigma_u = 1445$ MPa.

Vickers hardness values measured on the sintered samples are presented in Table 3. The obtained data for compressive strength demonstrate increased mechanical properties for samples S2 and S3. However, in contrast, sample S3 exhibits a higher hardness value of $\cong 10.5$ GPa (1072 *HV*) compared to S1 and S2 manifesting $\cong 6.7$ GPa (689 *HV*) and 6.5 GPa (677 *HV*), respectively.

4. CONCLUSIONS

The composites of the Ti_3SiC_2–TiC–$TiSi_2$ were synthesized by sintering the initial powder mixtures Ti–Si–C system. The relationship between the parameters of the sintering process and the mechanical properties of composite materials was studied. Relatively low strength values of sample S1 ($\sigma_u = 1096$ MPa) may be due to the insufficient duration of the sintering process, which did not ensure the full formation of interfacial bonds and led to residual porosity. As a result, this led to relatively low mechanical-property values. In contrast, sample S2 demonstrated the best combination of strength and hardness ($\sigma_u = 1460$ MPa, hardness $\cong 6.5$ GPa). This improvement is attributed to the two-stage sintering process, where initial heating and cooling helped relax residual stresses, while re-sintering enhanced diffusion processes, reduced structural defects, and promoted a more homogeneous microstructure. It was found that sample S3 has a higher hardness ($\cong 10.5$ GPa) compared to S1 and S2 due to the increased sintering pressure (90 MPa). These factors contributed to increased densification of the composite and enhanced interaction between the matrix and the constituent phases.

ACKNOWLEDGEMENT

This work was partially supported by the project No. 056/26 of the G. V. Kurdyumov Institute for Metal Physics of the N.A.S. of Ukraine.

AUTHORS' CONTRIBUTIONS

I.M.K.: conceptualization, x-ray investigation, writing review and

editing; A.M.L.: SPS sintering, writing review and editing; M.A.S.: electron-microscopy studies, formal analysis; S.O.K.: mechanical testing, formal analysis; O.V.Z.: mechanical testing, formal analysis; T.O.M.: electron-microscopy studies, formal analysis; I.V.G.: preparation of samples for mechanical tests; O.D.R.: conceptualization, supervision, writing review and editing.

REFERENCES

1. I. M. Low, *Advances in Science and Technology of $M_{n+1}AX_n$ Phases* (Woodhead Publishing: 2012).
2. M. Naguib, M. Kurtoglu, V. Presser, J. Lu, J. Niu, M. Heon, L. Hultman, Y. Gogotsi, and M. W. Barsoum, *Adv. Mater.*, **23**: 4248 (2011).
3. M. Sokol, V. Natu, S. Kota, and M. W. Barsoum, *Trends. Chem.*, **1**: 210 (2019).
4. S. Haji Amiri, and N. Pourmohammadie Vafa, *Synthesis and Sintering*, **1**, No. 4: 216 (2021).
5. T. Chen, P. M. Green, J. L. Jordan, J. M. Hampikian, and N. N. Thadhani, *Metall. Mater. Trans. A.*, **33**: 1737 (2002).
6. M. W. Barsoum and T. El-Raghy, *Adv. Mater. Proc.*, **7**: 51 (1997).
7. E. Tabares, A. Jiménez-Morales, and S. A. Tsipas, *Bol. Soc. Esp. Ceram. Vidr.*, **60**, Iss. 1: 41 (2021).
8. L. Silvestroni, C. Melandri, and J. Gonzalez-Julian, *J. Eur. Ceram. Soc.*, **41**, Iss. 12: 6064 (2021).
9. S.-B. Li, L.-T. Zhang, and L.-F. Cheng, *Mater. Sci. Technol.*, **18**, Iss. 12: 1494 (2002).
10. S. Li, L. Cheng, and L. Zhang, *Mater. Sci. Eng. A.*, **341**, Iss. 1–2: 112 (2003).
11. S. L. Yang, Z. M, Sun, H. Hashimoto, Y. H. Park, and T. Abe, *Oxid. Met.*, **59**: 155 (2003).
12. L. Luterotti and S. Gialanella, *Acta Mater.*, **46**, Iss. 1: 101 (1998).